J Nanostruct 15(1): 134-149, Winter 2025

RESEARCH PAPER

New Approach to in situ Chemical Vapor Deposition-Grown Graphene reinforced Copper Matrix for Increasing Electrical Conductivity and Mechanical Properties

Misagh Alaie Faradonbeh [1], *Alimorad Rashidi* [1]*, *Zohal Safaei Mahmoudabadi* [1], *Fatemeh Dodangeh* [2]

[1] *Nanotechnology Research Center, Research Institute of Petroleum Industry, Tehran, Iran*

[2] *Department of Chemistry, Science and Research Branch, Islamic Azad University, Tehran, Iran*

ARTICLE INFO

Article History:
Received 21 September 2024
Accepted 19 December 2024
Published 01 January 2025

Keywords:
Chemical Vapor Deposition (CVD)
Copper-graphene nanocomposites
Copper wire
Electrical Conductivity
Graphene
Mechanical Properties

ABSTRACT

The chemical compatibility and successful formation of morphology of graphene sheet growth on the copper matrix were investigated with scanning electron microscope (SEM) techniques, transmission electron microscopy (TEM), EDS and mapping analysis tests, RAMAN spectroscopy, X-ray diffraction (XRD). Also, the effects of individual process variables such as 0 to 900 cc/min methane gas flow rate, 0 to 45 minutes, and 1000 °C are used in CVD method to grow the graphene on Cu substrate and as a result of electrical conductivity and mechanical properties were evaluated for different outcomes samples in this reasearch. The results revealed to the optimum values for Cu powder/Gr nanocomposite samples were found at 300 cc/min methane flow rate during 45 minutes at 1000 °C, as well as 0.2 mm thickness of Cu wire in the same condition which led these samples to high electrical conductivity, and high hardness rather than Cu pure. The great instruction of graphene growth design and morphology is the cause for increasing electron mobility in the Cu/graphene nanocomposites. As a result, the electrical conductivity of the Cu/Gr nanocomposites is three times higher than the counterpart without graphene growth. Also, the outcomes of this research were found the highest amount of electrical conductivity and hardness value of Cu/Gr nanocomposite are more than other Cu/Gr composites. This study provides a new approach for modification Cu substrate by growth graphene using CVD method in order to high electrical conductivity and high mechanical properties.

How to cite this article
Alaie Faradonbeh M., Rashidi A., Safaei Mahmoudabadi Z., Dodangeh F. New Approach to in situ Chemical Vapor Deposition-Grown Graphene reinforced Copper Matrix for Increasing Electrical Conductivity and Mechanical Properties. J Nanostruct, 2025; 15(1):134-149. DOI: 10.22052/JNS.2025.01.013

INTRODUCTION

The electrical conductivity in the metals generally uses the metallic bonds and the free electrons for the transportation of the electric energy. With the development of electric power, and electronics, copper conductor is required to be light, strong, highly conductive and high current-carrying. One of the problems in electrical power systems (transmission and distribution lines) is the loss of energy and it will be around twenty percent of total energy per year [1–4]. Although, the alloy compounds are not free from some defects. One of which is their low resistance to the aggressive influence of environmental factors such as oxygen,

* *Corresponding Author Email: Rashidiam@ripi.ir*

temperature, and electromagnetic radiation. In addition, the class of materials as the complex iron oxides with outstanding electronic properties that are favorable for practical application [5–17].

In this new century, copper (Cu) is one of the important metals which is used in different instruments such as integrated circuits, electronic packages, and electric switches, due to recognizable features such as high electrical conductivity, fatigue resistance, workability, and corrosion resistance. However, Cu has limited mechanical properties. Different composites of copper are analyzed by some researchers [4–6] to help them to proud useful applications. Matrix composites of the metal-reinforced with new instruction include particles displays composition of properties their main materials, which is illustrated modify properties that are compared with the main matrix. Different groups of scientists discussed instruction of metal matrix composite [7–23]. Producing new material with high mechanical and electrical virtues need to produce a microstructure in which displacement movements are closed and dispersion of free electrons is increased [24–28].

Many studies have been investigated to fabricate carbon-based nanocomposites in order to improve electrical conductivity and mechanical properties. Chinnappan et. al. [29] studied the fabrication of MWCNT/Cu nanofibers based on electrospinning method as a result of the electrical conductivity is rising 1.479 S cm^{-1}. Mu Cao et. al. [30] investigated the Cu/Gr nanocomposite based on CVD method as a result of the electrical conductivity is rising to 68.2×10^{6} sm^{-1}. Recently, Cu/Gr nanocomposites have received considerable attention as alternative volunteer in electrical device applications with high electrical conductivity such as conductive wires or tracks, lead frames, cables and pantographs which explains its abundance in many applications ranging from microelectronics, overhead power transmission lines, active heat exchangers to heat sinks [31-33]. Also, several experimental investigations showed that graphene-reinforced metal composites have higher strengths in combination with lighter weights, compared with conventional metals and composites which are used for various applications such as photocatalysts, energy storage, nanoelectronics, batteries, and abrasion resistant materials [31,34-36].

The allotrope of carbon is graphene (G) and it is a single layer or a few layers of covalently bonded sp2 carbon atoms, hexagonally packed in a structure like a honeycomb crystal [37-41]. Graphene has conductivity value 1.4 times more than copper. So, that is expected the reinforcement instruction of fabricating metal matrix composites make high thermal conductivity. Although, some practical properties such as the type of graphene and some parameters in producing graphene have some results to doubt the thermal conductivity of graphene/metal matrix composites. Additionally, the graphene layer which is grown on the copper matrix can make high electrical conductivity and electron mobility. Capability to decrease transferring of displacement and connection between graphene and copper materials to has good bonding that is a result of density trend and little moist conducting graphene and copper [42]. The best economical and practical way for the growth of graphene on metal such as Ni [43], Pd [44], Ru [45], Ir [46] , or Cu [47] is the CVD method. More, in new researches, growing the single-layer deposition of 2Dimensional (D) graphene on copper on huge areas produces new materials with high quality with different applications [47-49].

The chemical vapor deposition (CVD) is a good method for growing graphene on copper metal and it can make the grain size of Cu substrate and improve its thermal features [50]. Graphene could enhance the conductive property of resin in graphene/polymer composites [51]. However, additional factors in producing graphene are cussed of confusing analyzing of thermal conductivity in this kind of composite and some results of researches show the negative effect of growing graphene on metal for thermal conductivity [52-54].

Changing the electrical conductivity of copper is one of the important issues in electrical power systems nowadays [55,56]. Electrical wire and cable were made of copper materials. These kinds of wires and cables are used in transmission and distribution lines in electrical power systems. The CVD method is chosen to make a new synthesis with a growing graphene layer on wire and copper materials [57,58].

In this work, we report for the first time the synthesis of Cu/Gr nanocomposite via CVD method in order to improved electrical conductivity and mechanical properties. Herein, the economical and available strategy is considered to grow

the graphene. The optimum condition reaction such as methane flow rate, time, and thickness of Cu substrate for graphene growth, electrical conductivity and mechanical properties were evaluated. We also proposed the graphene growth mechanism on Cu substrate and explained the role of methane gas in the CVD process. The results are promising for future applications of Cu/Gr composites for electronic devices, electronic wire, cable network, electrical line, transmission line and distribution lines in electrical power system.

In this research, Cu powder/Graphene (Gr) nanocomposites with high electrical conductivity (145×10^6 $S.m^{-1}$) and high mechanical properties (72 shore d) was fabricated by CVD method (300 cc/min methane flow rate, 1000°C, 45 min).

MATERIALS AND METHODS

Chemicals and reagents

In this work, different materials and gases are used. The copper wire (0.2, 0.3, 0.8 and 1.5 mm) are used. Also, Copper powders (the purity of copper powder: 99.90 %) is used in this research. Methane gas with 99.99% purity and hydrogen gas with 99.99% purity are used in this research.

Graphene growth

Atmospheric pressure (AP) annealing and CVD graphene growth

The atmospheric pressure CVD graphene growth procedure is described as follows:

In brief, substrates (copper wire or copper powder) were annealed under 200 cc/min flow of hydrogen gas at 1000 °C. After the annealing step, methane gas is introduced to the reactor at a different rate of gas flow with different times and variable ramps (cc/min) to grow a continuous graphene film. Finally, the product is obtained after the furnace is gradually cooled down (Fig. 1).

Thermal annealing has been widely employed as one of the experimental control knobs for a number of condensed matter systems, and graphene is no exception. Thermal annealing has been extensively used for graphene on various substrates in order to remove any possible contamination and thus improve sample cleanliness [59,60].

Characterization

A scanning electron microscope (SEM), all pictures were taken with MIRA III microscope device that is a product of TESCAN Company, this instrument is using an accelerating voltage of 15 kV. A high-resolution transmission electron microscope (HRTEM) was carried out on an FEI Titan 300 microscope with an accelerating voltage of 120 kV. TEM device is manufactured by the Netherland and the model of this device is: CM120 and the maximum voltage of this device is 100 kV. The X-ray diffraction (XRD) patterns (Siemens, model D5000) using an X-ray diffractometer were determined with Cu Kα radiation (λ=0.154 nm, 40 kV, 100 mA). Raman instrument that is working with a micro-Raman spectrometer, manufacture by the Teksan company (device's model: TakRam N1-541), with an exciting wavelength of 532

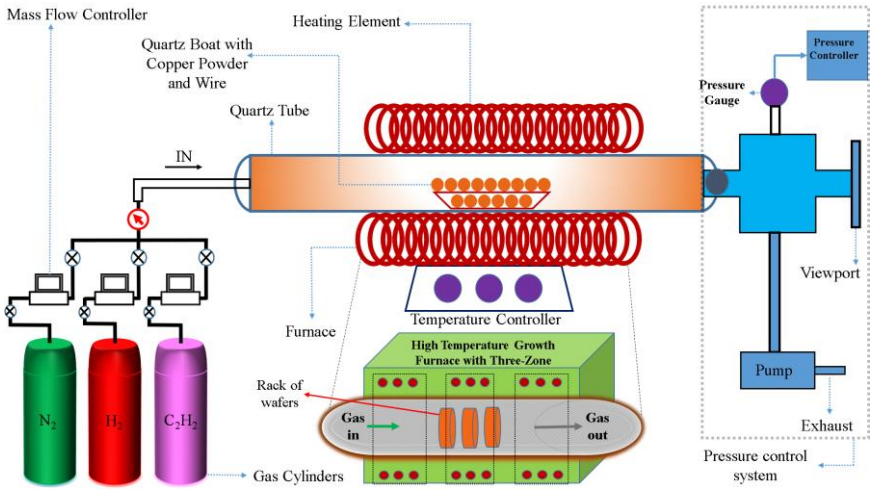

Fig. 1. Schematic reactor setup for CVD method for synthesis of Cu /Gr nanocomposite

nm. In addition, HIOKI 3522 LCR HiTESTER is the advanced device to measure resistance. Also, the flexural strength of the Cu/Gr nanocomposites was performed with cuboid testing samples based on ASTM B528-12 standard with 30 mm length, 8 mm width and 6 mm thickness, respectively [61].

RESULTS AND DISCUSSION

Characterization of Cu powder/Gr and Cu wire/Gr nanocomposite

Fig. 2a show the Raman spectrum of Cu powder, and graphene grown on a Cu powder. As it seen a typical Raman spectrum of graphene has three major features: (i) the D band at ~ 1338.164 cm^{-1} related to only a small amount of defects on the graphene surface (ii) the 2D-band at ~2919.574 cm^{-1} corresponded to the double resonance Raman scattering process, and (iii) the G-band at ~1600cm^{-1} that comes out of the in-plane vibrations of sp^2-hybridized carbon atoms near the Γ point [62,63], and when it compares with the Raman spectrum of the copper without the layer of graphene, this proves that the appearance of G-band and 2D-band demonstrated the successful growth of graphene on the copper powder during of CVD procedure. Furthermore, the first-order boundary belongs to the D-band of graphene. Also, it is presented lowing defect-induced area boundary phonons and can be disregarded from the spectra. As result, offering that the incorrect arrangement and defects of interdomain expansion were small and unimportant. In addition, Raman test in Fig. 2c shows graphene growth in Cu wire sample and these results described the signal of graphene related to these peaks; D (1348.837 cm^{-1}), G (1605.132 cm^{-1}), and 2D band (2938.33cm^{-1}). Also, as reported in the articles [36,64], the raman quality of graphene formed in nanocomposites is weaker than that of pure graphene. Because the intensity of the 2D-band in nanocomposite is somewhat lower than the intensity in pure graphene, which indicates the growth of graphene

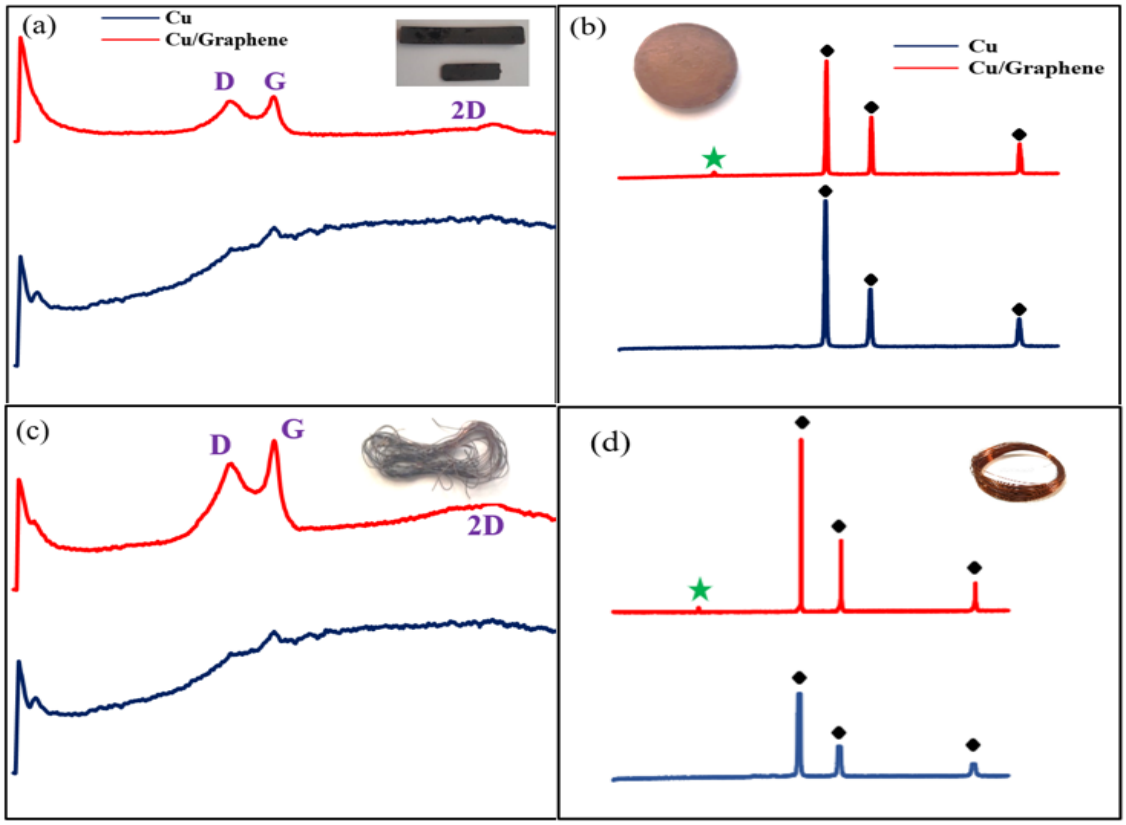

Fig. 2. (a) Raman spectra of Cu powder/Gr nanocomposite, (b) XRD patterns of Cu powder/Gr nanocomposite, (c) Raman spectra of Cu wire/Gr nanocomposite, and (d) XRD patterns of Cu wire/Gr nanocomposite

in the nanocomposite substrate. For more prove, The XRD pattens is taken from pure Cu, Cu powder/Gr, and Cu wire/Gr nanocomposite are shown in Fig. 2b, and 2d. In the X-ray diffraction model includes the graphene nanosheets composite, only Cu and graphene phases are detected in this samples. In XRD pattern one extra peak has appeared at 25° and this peak is related to formation of layers of graphene in instruction of nanocomposites. This peak shows the growth of graphene on Cu substrate. According to Fig. 2d., in XRD of Cu pure and nanocomposites according to ICDD card (85-1326), at 2θ = 43, 50.15 and 73.9 which correspond to (111), (200), (220), are regarding to copper metal. Also, in Fig. 3d., at 2θ = 43.2, 50.3, 74.15, which according to (111), (200), (220) and graphene peak at 2θ = 25° which related to Cu wire/Gr nanocomposite. Thus, the patterns indicate that layers of graphene are grown on Cu substrates during CVD procedure.

The morphology of Cu/Gr nanocomposite in Fig. 3 shows similar sheet morphology for nanoparticles and accretion can be seen in these samples. The magnification micrograph are illustrated the morphology of graphene growth on the Cu surface. As it shown the morphology and size of graphene sheets were changed with the flow and time of methane gas which pass on copper powder in furnace. FESEM images show our sample Fig. 3a-c with the graphene growth procedure that include variable time of flow of methane gas 15, 30 and 45 minutes and constant flow of methane gas (CH_4 = 300 cc/min) has been investigated in this part of article. Furthermore, this clear in Fig. 3c, morphology of graphene formation has the best instruction and the diameter of particles in this sample is from 100 nm to 140 nm. Additionally, there are other samples in Fig. 3d-f with different flow of methane gas 150, 450 and 900 cc/min with the same time of methane gas flow 45 minutes and the best morphology of graphene instruction has seen in Fig. 3e. Graphene formation in the best samples are more particle overlap and more adhesion and

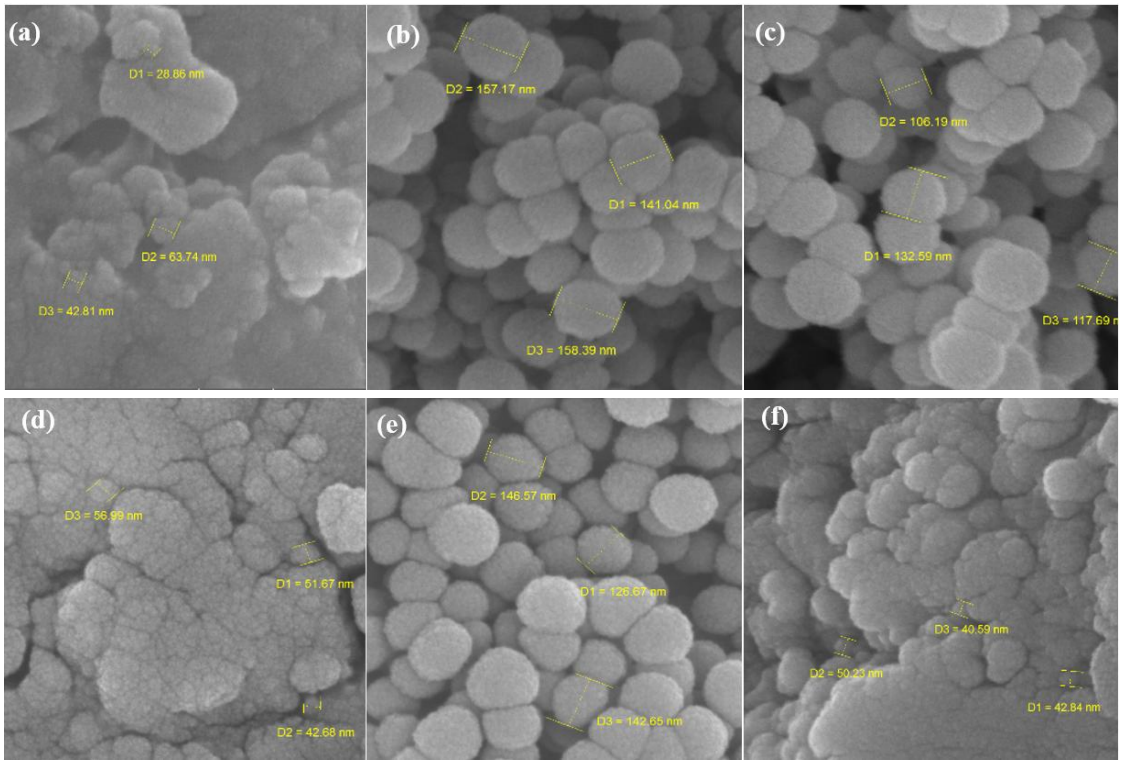

Fig. 3. Nanocomposite Cu/Gr; (a) CH_4 = 300 cc/min, 15 minutes passing flow of CH_4 gas on copper powder; (b) CH_4 = 300 cc/min, 30 minutes passing flow of methane gas on copper powder; (c) CH_4 = 300 cc/min, 45 minutes passing flow of CH_4 gas on copper powder; (d) CH_4 = 150 cc/min, 45 minutes passing flow of CH_4 gas on copper; (e) CH_4 = 450 cc/min, 45 minutes passing flow of CH_4 gas on copper powder; (f) CH_4 = 900 cc/min, 45 minutes passing flow of CH_4 gas on copper powder

bonding between boundaries of graphene sheet particles, which are compared with other FESEM sample images. Therefore, conducting frame in nanosphere graphene particles are more useful for electron transferring and electrical conductivity. Additionally, the formation of graphene on the Cu powder in this nanocomposite is more regular and with less porosity which is compared with other sample and as a result of helpful to make high electrical conductivity with low resistance [65]. Thus, the effects of individual process variables such methane gas flow rate, time, and temperature are used in CVD method to grow the graphene on Cu substrate in order to controllable and rational process [66,67].

The SEM-EDX mapping of Cu powder/Gr nanocomposite is showed in the Fig. 4. From these images, the presence of carbon, oxygen, and Cu in this nanocomposite can be seen. Another ability of X-ray mapping in EDX technique is indicating the pictures with unique colors which presented different elements and theirs dispersion. The maps of expanding of some elements such as C, O, and Cu are displayed exclusively and similarity with the main image as illustrated in the Fig. 4. The map of elements survey shows that the most active elements like Cu and C were regularly distributed throughout the nanocomposite.

Also, In EDS analysis, sharp peak of carbon is appeared and this is regarding to formation of surface of graphene on copper powder in CVD process.

Electrical wires need to change to new one because of cost, weight, ability for transferring electrical energy or heat transferring or wire strength. FESEM images show our sample a and b in Fig. 5 include two different wire 0.2 mm and 0.3 mm with graphene growing on it during CVD procedure with flow of methane gas 300 cc/min and time 45 minutes. As it shown in Fig. 5 graphene is grown on copper wire with good formation and, the best morphology of graphene instruction has been seen in these figures with the high density of graphene particles growth with maximum overlap at the boundaries of particles that has excellent effect to change the electrical conductivity.

EDS/MAPPING analysis are shown in Fig. 6 for Cu wire/Gr nanocomposite .The sharp peak of carbon is appeared and this is regarding to formation of surface of graphene on copper wire and also, uniform dispersion carbon in the nanocomposite is revealed .

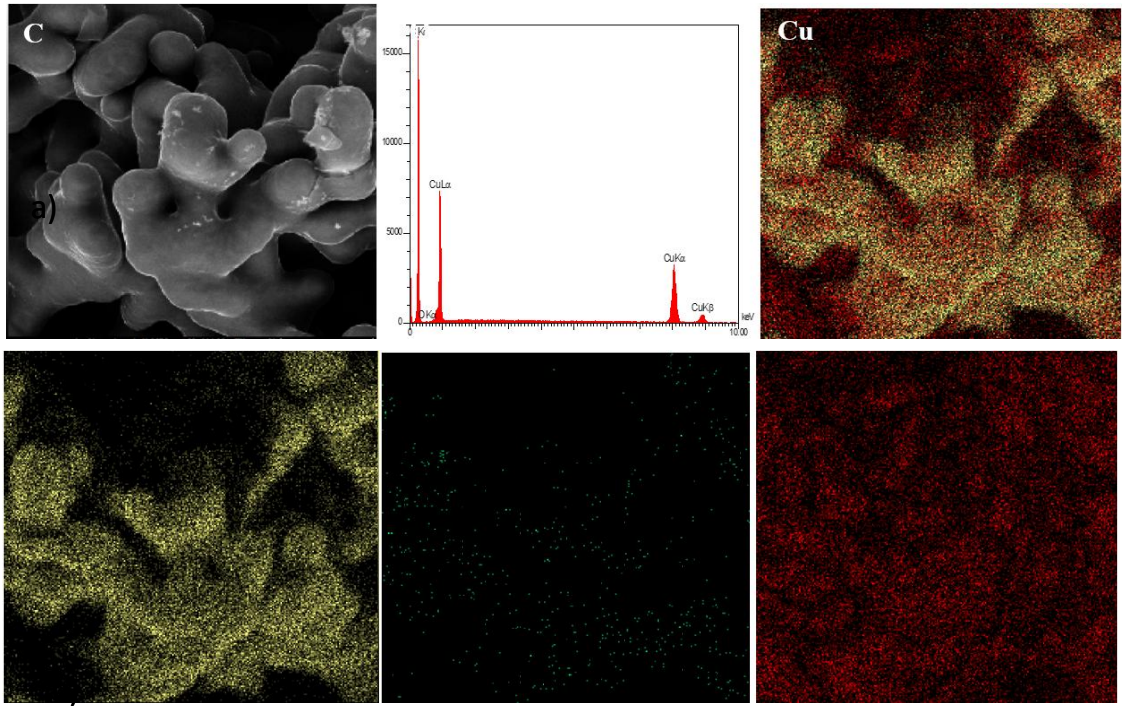

Fig. 4. SEM/EDX mapping with scale bar 10µm from Cu powder/Gr sample, C, O and CU elements image.

TEM images from Cu powder/Gr nanocomposites is shown in Fig. 7a. It can be observed that the heavier element is copper pure which is darker and another element is graphene that is lighter and brighter. All of these TEM images show copper metal and graphene compose together and these images prove this issue correctly and completely.

Also, in TEM images that graphene is composed and growth on copper wire (Fig. 7b). The big and thin layers of graphene with prevalent corrugated organization (effect of the overlapping graphene margin) are investigated. As received the results of TEM images, similar spread of graphene in Cu particle surface. Additionally, it is shown in these images changing density and it is caused to have variable value of electrical conductivity in different samples. More, these images prove that graphene has sheet morphology with excellent crystallinity on copper surface. These TEM images in Fig. 7b show the composed between the shell/ nanoparticles, the lighter parts include graphene and interior/pores, the darker parts include copper metal. Also, results indicate that the graphene layers are well dispersed in the Cu /Gr nanocomposites.

Electrical conductivity and Hardness of the Cu /Gr nanocomposites

The value of electrical resistivity is measured by HIOKI 3522 LCR HiTESTER which is the ~~Japanese~~ advanced device to evaluate resistance and this resistance meter has the ability to measure resistivity up to three decimals. Electrical conductivity is the inverse of electrical resistivity in this research and this means that increasing of electrical resistance causes of decreasing of electrical conductivity. Additionally, pure copper powder (%98 product of Germany) is used in this research and the electrical conductivity of

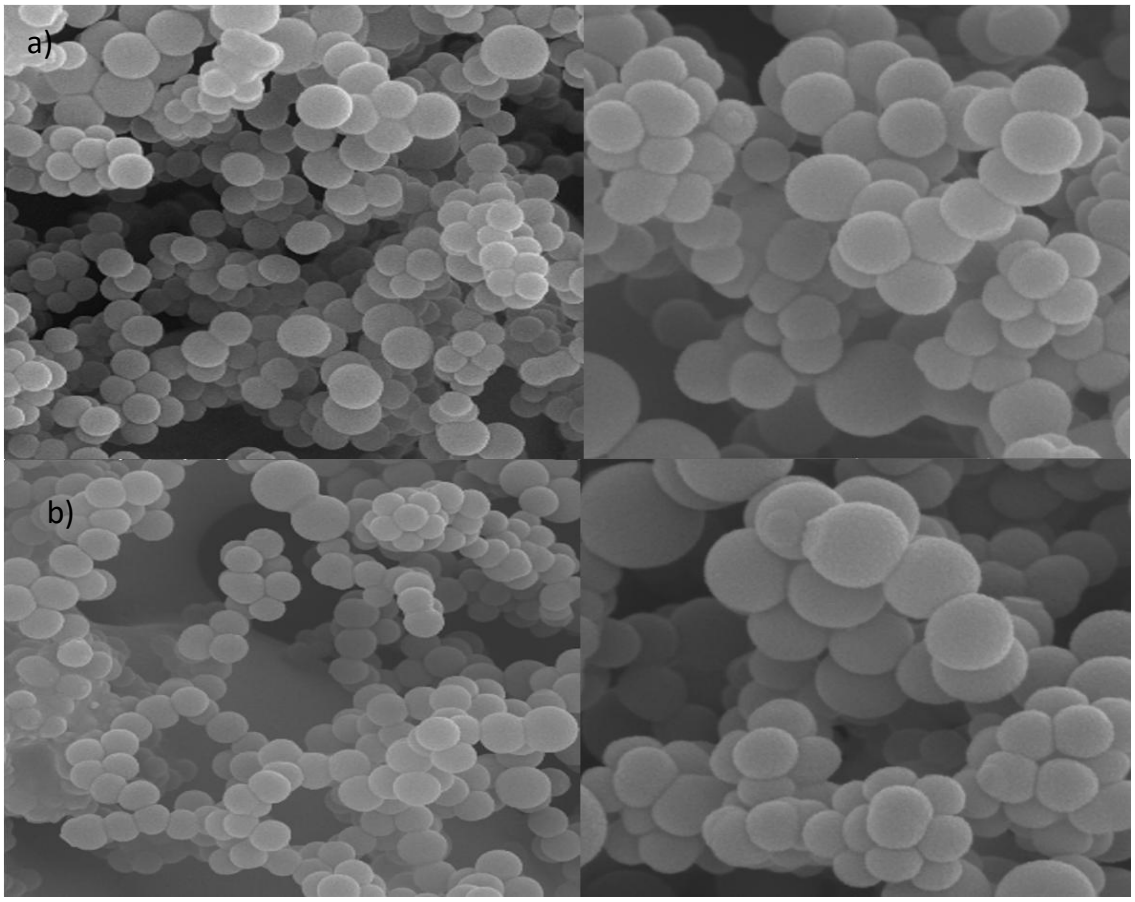

Fig. 5. Nanocomposite Cu wire/Gr, CH_4 = 300 cc/min and 45 minutes passing flow of CH_4 gas on copper wire; (a) Wire 0.2 mm; (b) Wire 0.3mm

pure copper is 58×10^6 sm^{-1}. Therefore, changing of electrical resistivity in composite of copper powder with growing layer of graphene and copper wire with growing layer of graphene in different samples, can change the value of electrical conductivity which has the inverse relationship comparing with changing of electrical resistivity.

The device of resistance meter exists at the research institute of petroleum industry, Tehran, Iran. Finally, if electrical resistivity is decreasing in this research, then the electrical conductivity is increasing in this research with the same inverse rising and reducing rate compared with electrical resistivity.

Electrical conductivity = (1/Electrical resistance)

Electrical resistivity and conductivity formula:
Resistivity:

$$\rho = R\frac{A}{L} \quad (1)$$

R: Electrical Resistance
A: Cross section area
L: Length

Conductivity:

$$\sigma = \frac{1}{\rho} \quad (2)$$

$$\sigma = \frac{L}{R\times A} \quad (3)$$

$$\sigma = \frac{1}{R}\times\frac{L}{A} \quad (4)$$

All of the samples are different in the process of graphene growth and structure of graphene which is composed on the surface of copper. But the length and the area of samples are same for all of them which are compared together. As a result, in electrical conductivity formula (L/A) is the constant value for all samples that are compared together and it has no effect on our analysis in this research. Therefore, the following formula is used in this research for our analysis:

$$\sigma = \frac{1}{R} \quad (5)$$

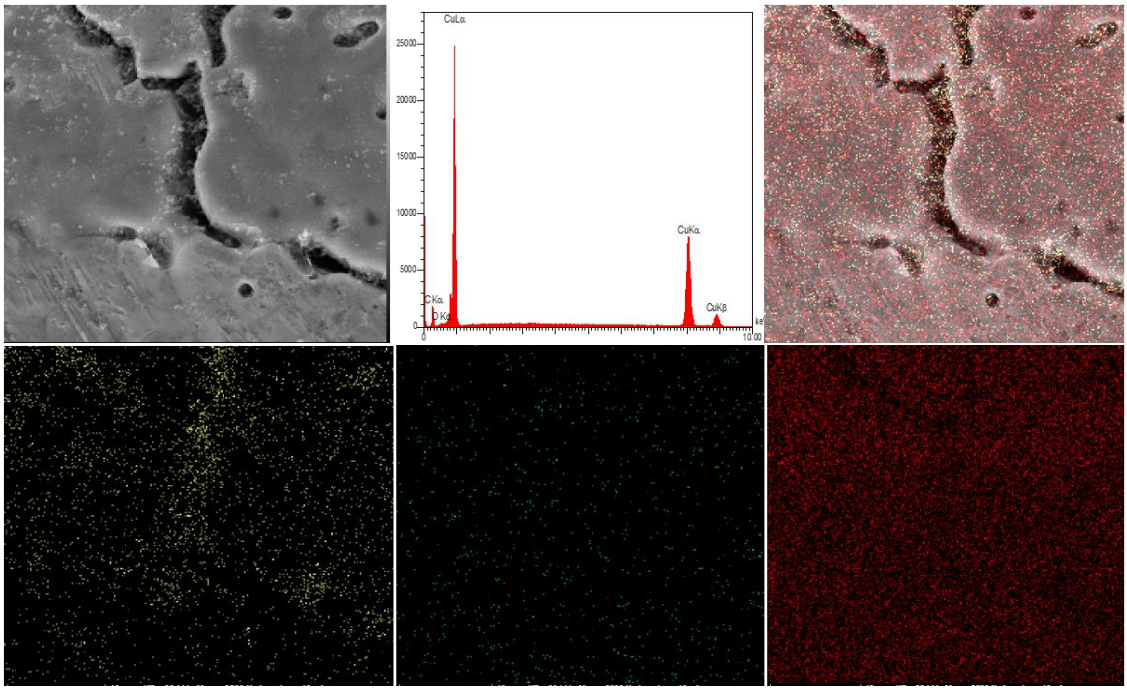

Fig. 6. SEM/EDX mapping with scale bar 10µm from Cu wire/Gr sample, C, O and Cu elements image.

The hardness value is measured by the hardness measuring device, this device measures the impact of the needle hitting the sample vertically and the measuring of this device is very sensitive, the device is available at the research institute of petroleum industry, Tehran, Iran.

Fig. 8 were caried out to evaluate electrical conductivity and hardness of Cu powder/Gr nanocomposites. As it is illustrated in Fig. 8a, formation of graphene layers have different hardness and electrical conductivity value when the variable ranges of flow of methane gas are used during graphene growth procedure. Electrical conductivity is increasing when the flow of methane gas is increased to 300 cc/min during 45 minutes, it is cause of the formation of graphene growth layers rising with increasing flow of methane gas. However, electrical conductivity rate is decreased when the flow of methane gas is increased more than 300 cc/min. Thus, the increasing flow rate of methane gas is the reason for decreasing residence time and as result, graphene growth is reduced and this leads to decreasing the electrical conductivity.

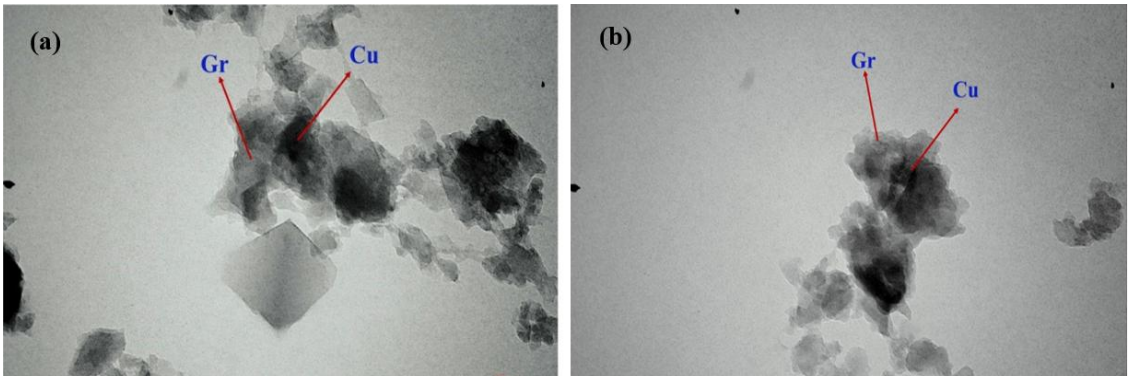

Fig. 7. (a) TEM images of Cu powder /Gr nanocomposite, and (b) TEM images of Cu wire/Gr nanocomposite

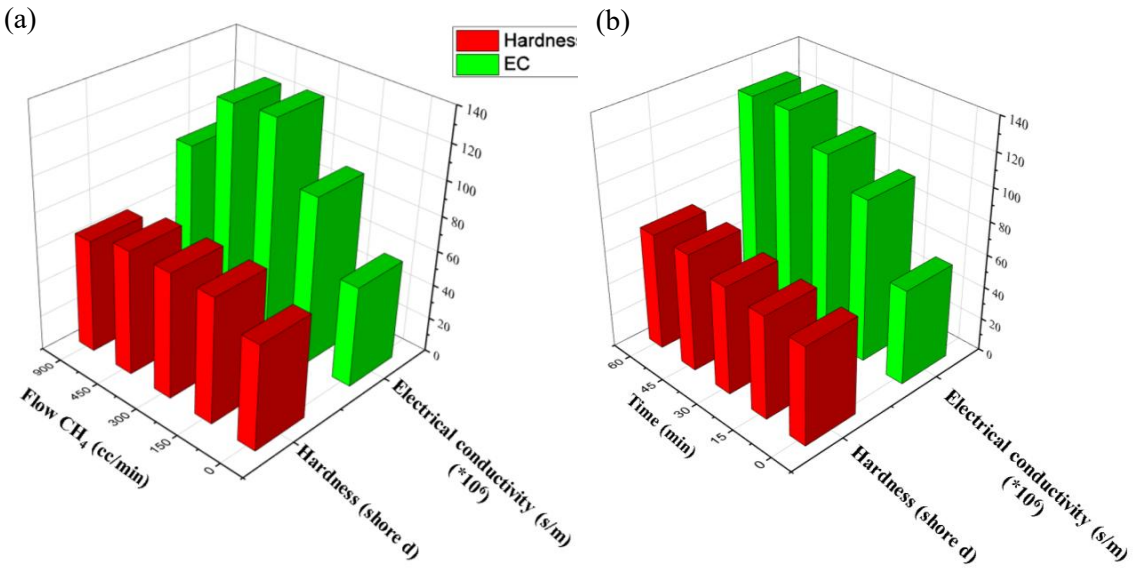

Fig. 8. Electrical conductivity and hardness of Cu/Gr nanocomposite (a) with various flow CH_4 at 45 minutes (b) with various time at 300cc/min

The synthesized nanocomposites have different structure and formation of graphene growing and best one is the sample with the flow of methane gas in range of 300 cc/min during 45 minutes because of complete formation excellent structure of graphene growth in the nanocomposite which lead to more electron transferring as a result of the best conductivity when it compared with other nanocomposites with different growing graphene. In fact, there is direct relationship between formation and instruction of graphene growth and electrical conductivity, it is because of higher density of graphene particles and more overlap of graphene particles and more contact of sheet graphene at their boundaries [68]. In addition, it is clear that the best hardness results of synthesized nanocomposite are created in the 300 cc/min flow of methane gas. The best hardness amount is created because of maximum formation of graphene layers and influence of those layers on Cu substrate and also it is increasing the hardness feature in nanocomposite.

Growing graphene on our Cu substrate is helpful to rise the hardening feature. One reason is the density of nanocomposites and overlapping edges of sheet graphene which is composed with Cu.

Table 1. Test results of flexural strength of 28 days Cu powder/Gr nanocomposites, other impurity for sample RGO-900 is 0.60.

NO	Name	Condition	Flexural Strength (MPa)
1	Cu	-	128.80
2	Cu/Gr nanocomposites	150 cc/min methane flow rate, 45 minutes, and 1000 °C	128.86
3	Cu/Gr nanocomposites	300 cc/min methane flow rate, 45 minutes, and 1000 °C	129.83
4	Cu/Gr nanocomposites	450 cc/min methane flow rate, 45 minutes, and 1000 °C	129.75

Table 2. Electrical conductivity and hardness for different types of Cu wire/Gr nanocomposite.

Material	Flow (cc/min)	Time minutes	Thickness (mm)	Electrical conductivity (s/m), ($\times 10^6$)	Hardness Shore d
Cu wire	-	-	0.2	23.02	26.5
Cu wire-1/Gr composite	300	30	0.2	68.83	27.6
Cu wire-2/Gr composite	300	45	0.2	99.07	27.67
Cu wire	-	-	0.3	24.53	26.2
Cu wire-3/Gr composite	300	30	0.3	49.06	27.5
Cu wire-4/Gr composite	300	45	0.3	57.45	27.58
Cu wire	-	-	0.8	28	25.8
Cu wire-5/Gr composite	300	30	0.8	42	27
Cu wire6/Gr composite	300	45	0.8	46.72	27.4
Cu wire	-	-	1.5	33.75	25.5
Cu wire-7/Gr composite	300	30	1.5	34.02	26.2
Cu wire-8/Gr composite	300	45	1.5	38.32	26.8

Additionally, the distribution of sheet graphene in Cu/Gr nanocomposites is found homogeneous in this research rather than the disordered particles. Reposition of displacement at the interfaces after composing, that is caused by the obstruction effect of graphene in nanocomposites, and leads to an increase in the strength, and hardness .

In Fig. 8b, the effect of time of methane gas pass is investigated over the electrical conductivity and hardness and it can be seen the best time for establishing of growing graphene layers is 45 minutes. At this time graphene layers are completely grown on Cu powder. When time is passing until 45 minutes, the methane gas is decomposed and graphene is formed, however when the time is passed after 45 minutes, there is no effect in graphene layers formation.

Also,flexuralstrengthofofCu/Grnanocomposites before and after growing graphene is tested for 28 days and all the results are tabulated as shown in (Table 1). The effect of growing graphene on the flexural strength of nanocomposites can be observed. As the results demonstrate that the graphene particles fill the porosity and space between the Cu particles with high adhesion and make this composite stronger to resist tearing in curvature and high flexural.

As it presented in the (Table 2) the value of electrical conductivity of wires with different diameters include the graphene layer is decreased when the amount of wire diameters is increased. Furthermore, the hardness value is decreased when wire diameter is increased. The value of hardness in all those wires are changed and they

Table 3. Comparison of electrical conductivity and hardness value over different composite.

Materials	Method	Electrical Conductivity (S/m)	Hardness Shore d	References
Cu (solid copper)	-	58×10^6	60	[69]
Cu/Gr composite	Friction stir processing	56.49324×10^6	23	[70]
Cu powder/Gr composite	Mixing Method Ultrasound, CVD	57.1×10^6 55.3×10^6 56.2×10^6	17 21.5 22.5	[33]
Cu/Gr composite	CVD	68.2×10^6	-	[71]
Printed copper patterns	Graphene coatings	0.0156±0.0048	-	[72]
Cu powder/Gr composite	CVD	145×10^6	72	In this work
Cu wire/Gr composite	CVD	99.07×10^6	27.67	In this work

are more than hardness value of copper wires when the graphene is growing on them. The reason for decreasing the amount of electrical conductivity in bigger diametre wires is low amount of graphene growth on those wires and decreasing growing of graphene on those wires. Thus, the best sample is Cu wire2/Gr nanocomposite with size 0.2 mm diameter which has best conductivity and hardness.

In order to investigate the electrical conductivity and hardness value of the recently progressive composites, based on Cu [71-74] are compared, as demonstrated in (Table 2) [75-77]. Based on the increasing electrical conductivity, hardness value, reaction temperature, and reaction time the developed Cu powder/Gr nanocomposites, and Cu wire-2/Gr nanocomposite might be elected as one of the most competitive nanocomposites among the Cu-based nanocomposites. Individually, CVD method is excellent for formation of graphene on Cu substrate because of using this method to grow the graphene on the substrate with carbone gas source and this process is using dispersion carbon source and breaking the carbon source (methane) on Cu metal surface [69,70].]Additionally, different setting and process to growth graphene on Cu surface such as flow of carbon source gas, time of passing the gas on the surface and temperature of furnace during this process, produce graphene with different structures on Cu surface and all FESEM and TM figures show these difference in structure with different compressions and adhesions of graphene particles which are mentioned in previouse paragraphs in this article. Additionally, Tauc method illustrates the effect of optical spectra and band gap of energy for different methods to analyze our samples in this research such as XRD, Raman, FESEM, TEM and SEM/EDX. UV-vis spectroscopy can measure optical spectra for several methods such as absorbance (A), transmission (T), reflectance (R) belong to the nature of material, nanomaterial and substrate. Tauc parameter which gives insight for the disorder in the film can demonstrate the Irregularities in the charts and graphs and justify the different colors in the photos by the value of light which is absorbed by material with different thicknesses [78-81].

Thus, the electrical conductivity and hardness are 145×10^6 sm^{-1} and 72 shore d for Cu powder/Gr composite sample in this work and 99.07×10^6 sm^{-1} and 27.67 shore d for Cu wire/Gr composite sample in this work respectively (Table 3).

CVD Mechanism for Growing graphene

Decomposition of methane source by CVD is the most popular method to produce large-area, high quality monolayer graphene on copper as the catalyst substrate [57,82,83]. Carbon atoms will nucleate and laterally expanded around the nucleus to form graphene areas with the decomposition of methane catalyzed by the copper at high temperature. The growing graphene process will be completed when the Cu substrate is fully covered by the graphene layer, which is related to the “self-limited surface deposition” growth mechanism [84,85]. On the other hand, decomposition of methane gas based on this

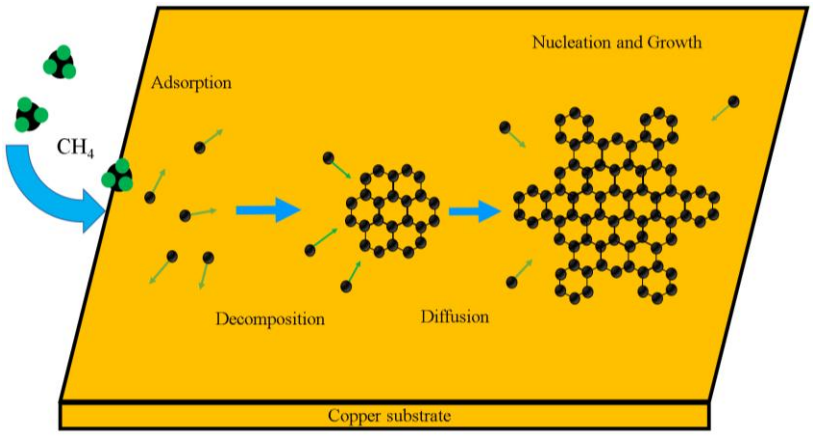

Fig. 9. Schematic of CVD graphene grown on Cu substrate

balance reaction $CH_4 \Leftrightarrow C.+2H$ carbon is grown on the Cu substrate [86,87]. Additionally, carbon with limit condensation on the copper substrate can be spread during the large area to some stabilized energetically region, result in hexagonal graphene zone is formed as Cu/Gr nanocomposites (Fig. 9). As discussed in this research, the flow rate of methane gas and passing the time of methane gas on Cu substrate as the setting of graphene growing in CVD procedure can change the formation, instruction, and volume of graphene is composed with Cu. Furthermore, adjusting the time and flow rate of methane gas are the cause of increasing the boundary and density of graphene sheet nanocomposites [88].

CONCLUSION

In summary, this work is presented growing graphene on Cu matrix to make copper powder/G and Cu wire/Gr composites with high electrical conductivity and improved hardness properties. For instance, the best one during different samples of Cu powder which is composed with the graphene through the adjusting CVD procedure system with passing flow of methane gas at 45 minutes on Cu substrate and with 300 cc/min flow of methane gas inside the furnace at 1000 °C has high electrical conductivity amount 145×10^6 sm^{-1} and hardness value 72 shore d when are compared with Cu pure electrical conductivity and hardness features that are 58×10^6 sm^{-1} and 60 shore d . Furthermore, the best sample of Cu wire/Gr composite is related to Cu wire 0.2 mm with synthesis setting of methane gas passing time 45 minutes and flow of 300 cc/min with excellent electrical conductivity 99.07×10^6 sm^{-1} and hardening feature 27.67 shore d. The morphology, instruction of graphene sheet, formation of composed graphene nanoparticles on Cu substrate, increasing the boundary between graphene grains, good compaction and adhesion of graphene particles formed on the copper surface and filling the empty space and gap between copper nanoparticles with graphene sheet and also using the CVD method as the best method for producing graphene with the maximum volume and amount of graphene on the large surface and area with various flow and time of carbon source gas are the reasons of changing the electrical conductivity and hardness properties to the high amounts. These results and outcomes of graphene growth procedure and formation of graphene sheet which is composed on Cu surface in this research are analyzed and proved with different exams and tests that are described completely in previous paragraphs.

ACKNOWLEDGMENT

This work supported by the Vice-presidency for Science and Technology of Iran, Center for International Science and Technology Cooperation (CISTC) and Research Institute of Petroleum Industry, Tehran, Iran (RIPI) for postdoctoral research program 2020-2021, under grant and project No. 92650019.

CONFLICT OF INTEREST

The authors declare that there are no conflicts of interest regarding the publication of this manuscript.

REFERENCES

1. Takata N, Lee S-H, Tsuji N. Ultrafine grained copper alloy sheets having both high strength and high electric conductivity. Mater Lett. 2009;63(21):1757-1760.
2. Hong E, Kaplin B, You T, Suh M-s, Kim Y-S, Choe H. Tribological properties of copper alloy-based composites reinforced with tungsten carbide particles. Wear. 2011;270(9-10):591-597.
3. Kumar S, Yadav A, Patel V, Nahak B, Kumar A. Mechanical behaviour of SiC particulate reinforced Cu alloy based metal matrix composite. Materials Today: Proceedings. 2021;41:186-190.
4. Spar J. Weather Analysis and Forecasting . vol. I, Motion and Motion Systems . Sverre Petterssen. McGraw-Hill, New York, ed. 2, 1956. 428 pp. Illus. $8.50.; Weather Analysis and Forecasting. vol. II, Weather and Weather Systems . Sverre Petterssen. McGraw-Hill, New York, ed. 2, 1956. 266 pp. Illus. $6. Science. 1956;124(3225):728-729.
5. Troyanchuk IO, Trukhanov SV, Khalyavin DD, Szymczak H. Magnetic properties of anion deficit manganites $Ln_{0.55}Ba_{0.45}MnO_{3-\gamma}$ (Ln=La, Nd, Sm, Gd, $\gamma\leqslant0.37$). J Magn Magn Mater. 2000;208(3):217-220.
6. Trukhanov SV. Investigation of stability of ordered manganites. Journal of Experimental and Theoretical Physics. 2005;101(3):513-520.
7. Rostami M, Majles Ara MH. The dielectric, magnetic and microwave absorption properties of Cu-substituted Mg-Ni spinel ferrite-MWCNT nanocomposites. Ceram Int. 2019;45(6):7606-7613.
8. Tishkevich DI, Grabchikov SS, Tsybulskaya LS, Shendyukov VS, Perevoznikov SS, Trukhanov SV, et al. Electrochemical deposition regimes and critical influence of organic additives on the structure of Bi films. J Alloys Compd. 2018;735:1943-1948.
9. Zubar TI, Fedosyuk VM, Trukhanov AV, Kovaleva NN, Astapovich KA, Vinnik DA, et al. Control of Growth Mechanism of Electrodeposited Nanocrystalline NiFe Films. J Electrochem Soc. 2019;166(6):D173-D180.
10. Zubar T, Trukhanov A, Vinnik D, Astapovich K, Tishkevich D, Kaniukov E, et al. Features of the Growth Processes and Magnetic Domain Structure of NiFe Nano-objects. The Journal of Physical Chemistry C. 2019;123(44):26957-

26964.
11. Darwish MA, Trukhanov AV, Senatov OS, Morchenko AT, Saafan SA, Astapovich KA, et al. Investigation of AC-Measurements of Epoxy/Ferrite Composites. Nanomaterials (Basel, Switzerland). 2020;10(3):492.
12. Algarou NA, Slimani Y, Almessiere MA, Alahmari FS, Vakhitov MG, Klygach DS, et al. Magnetic and microwave properties of $SrFe_{12}O_{19}/MCe_{0.04}Fe_{1.96}O_4$ (M = Cu, Ni, Mn, Co and Zn) hard/soft nanocomposites. Journal of Materials Research and Technology. 2020;9(3):5858-5870.
13. Yakovenko OS, Matzui LY, Vovchenko LL, Oliynyk VV, Trukhanov AV, Trukhanov SV, et al. Effect of magnetic fillers and their orientation on the electrodynamic properties of $BaFe_{12-x}Ga_xO_{19}$ (x = 0.1–1.2)—epoxy composites with carbon nanotubes within GHz range. Applied Nanoscience. 2020;10(12):4747-4752.
14. Kozlovskiy AL, Shlimas DI, Zdorovets MV. Synthesis, structural properties and shielding efficiency of glasses based on TeO_2-(1-x)ZnO-xSm_2O_3. Journal of Materials Science: Materials in Electronics. 2021;32(9):12111-12120.
15. Zdorovets MV, Kozlovskiy AL, Shlimas DI, Borgekov DB. Phase transformations in FeCo – Fe_2CoO_4/Co_3O_4-spinel nanostructures as a result of thermal annealing and their practical application. Journal of Materials Science: Materials in Electronics. 2021;32(12):16694-16705.
16. Kozlovskiy AL, Zdorovets MV. Effect of doping of $Ce^{4+/3+}$ on optical, strength and shielding properties of (0.5-x) TeO_2-0.25MoO-0.25Bi_2O_3-xCeO_2 glasses. Mater Chem Phys. 2021;263:124444.
17. Kozlovskiy A, Egizbek K, Zdorovets MV, Ibragimova M, Shumskaya A, Rogachev AA, et al. Evaluation of the Efficiency of Detection and Capture of Manganese in Aqueous Solutions of $FeCeO_x$ Nanocomposites Doped with Nb2O5. Sensors (Basel, Switzerland). 2020;20(17):4851.
18. Strayer-Scherer A, Liao YY, Young M, Ritchie L, Vallad GE, Santra S, et al. Advanced Copper Composites Against Copper-Tolerant Xanthomonas perforans and Tomato Bacterial Spot. Phytopathology®. 2018;108(2):196-205.
19. Palza H, Quijada R, Delgado K. Antimicrobial polymer composites with copper micro- and nanoparticles: Effect of particle size and polymer matrix. J Bioact Compatible Polym. 2015;30(4):366-380.
20. da Silva AB, Arjmand M, Sundararaj U, Bretas RES. Novel composites of copper nanowire/PVDF with superior dielectric properties. Polymer. 2014;55(1):226-234.
21. Prabu SB, Karunamoorthy L, Kathiresan S, Mohan B. Influence of stirring speed and stirring time on distribution of particles in cast metal matrix composite. J Mater Process Technol. 2006;171(2):268-273.
22. Kaczmar JW, Pietrzak K, Włosiński W. The production and application of metal matrix composite materials. J Mater Process Technol. 2000;106(1-3):58-67.
23. Arsenault RJ, Taya M. Thermal residual stress in metal matrix composite. Acta Metall. 1987;35(3):651-659.
24. Cann DP. Fundamentals of Materials Science: The Microstructure-Property Relationship Using Metals as Model Systems, 2nd Edition, by Eric J. Mittemeijer, Springer Nature Switzerland AG 2021. Journal of Materials Science. 2022;57(14):7127-7130.
25. Rossiter PL. The Electrical Resistivity of Metals and Alloys: Cambridge University Press; 1987 1987/04/24.
26. Fahimi N, Abachi P. The role of powder preparation route on physical and mechanical properties of Cu-rGO bulk nanocomposites. Materials Today Communications. 2021;28:102470.
27. Lee J-Y, Sohn Y, Kim HS, Han JH. Effect of dispersion and alignment of graphite fibers on thermal expansion induced fracture of graphite fiber/copper composite. Materials Today Communications. 2020;25:101450.
28. Zuo H, Wei W, Yang Z, Li X, Xie W, Liao Q, et al. Synchronously improved mechanical strength and electrical conductivity of Carbon/Copper composites by forming Fe3C interlayer at C/Cu interface. Materials Today Communications. 2021;28:102661.
29. Chinnappan A, Lee JKY, Jayathilaka WADM, Ramakrishna S. Fabrication of MWCNT/Cu nanofibers via electrospinning method and analysis of their electrical conductivity by four-probe method. Int J Hydrogen Energy. 2018;43(2):721-729.
30. Cao M, Xiong DB, Yang L, Li S, Xie Y, Guo Q, et al. Ultrahigh Electrical Conductivity of Graphene Embedded in Metals. Adv Funct Mater. 2019;29(17).
31. Goli P, Ning H, Li X, Lu CY, Novoselov KS, Balandin AA. Thermal Properties of Graphene–Copper–Graphene Heterogeneous Films. Nano Lett. 2014;14(3):1497-1503.
32. Zhang Q, Liu Y, Liao T, Zhang C, Wu X, Liu Y, et al. Graphene/Cu composites: Electronic and mechanical properties by first-principles calculation. Mater Chem Phys. 2019;231:188-195.
33. Wang M, Wang L-D, Sheng J, Yang Z-Y, Shi Z-D, Zhu Y-P, et al. Direct synthesis of high-quality graphene on Cu powders from adsorption of small aromatic hydrocarbons: A route to high strength and electrical conductivity for graphene/Cu composite. J Alloys Compd. 2019;798:403-413.
34. Iqbal AKMA, Sakib N, Iqbal AKMP, Nuruzzaman DM. Graphene-based nanocomposites and their fabrication, mechanical properties and applications. Materialia. 2020;12:100815.
35. Peng W, Sun K. Effects of Cu/graphene interface on the mechanical properties of multilayer Cu/graphene composites. Mech Mater. 2020;141:103270.
36. Hwang J, Yoon T, Jin SH, Lee J, Kim TS, Hong SH, et al. Enhanced Mechanical Properties of Graphene/Copper Nanocomposites Using a Molecular-Level Mixing Process. Adv Mater. 2013;25(46):6724-6729.
37. Ram B, Mizuseki H. Tetrahexcarbon: A two-dimensional allotrope of carbon. Carbon. 2018;137:266-273.
38. Sharma BR, Manjanath A, Singh AK. Pentahexoctite: a new two-dimensional allotrope of carbon. Scientific reports. 2014;4:7164-7164.
39. Mahmoudabadi ZS, Rashidi A, Tavasoli A, Esrafili M, Panahi M, Askarieh M, et al. Ultrasonication-assisted synthesis of 2D porous MoS_2/GO nanocomposite catalysts as high-performance hydrodesulfurization catalysts of vacuum gasoil: Experimental and DFT study. Ultrason Sonochem. 2021;74:105558-105558.
40. Safaei Mahmoudabadi Z, Rashidi A, Tavasoli A. Synthesis of two-dimensional TiO_2@multi-walled carbon nanotube nanocomposites as smart nanocatalyst for ultra-deep oxidative desulfurization of liquid fuel: Optimization via response surface methodology. Fuel. 2021;306:121635.
41. Mahmoudabadi ZS, Tavasoli A, Rashidi A, Esrafili M. Catalytic activity of synthesized 2D MoS_2/graphene nanohybrids for the hydrodesulfurization of SRLGO: experimental and DFT study. Environmental Science and Pollution Research. 2020;28(5):5978-5990.
42. Yang M, Weng L, Zhu H, Fan T, Zhang D. Simultaneously enhancing the strength, ductility and conductivity of copper matrix composites with graphene nanoribbons. Carbon. 2017;118:250-260.
43. Yao Q, Lu Z-H, Yang Y, Chen Y, Chen X, Jiang H-L. Facile

synthesis of graphene-supported Ni-CeOx nanocomposites as highly efficient catalysts for hydrolytic dehydrogenation of ammonia borane. Nano Research. 2018;11(8):4412-4422.
44. Ma D, Liu M, Gao T, Li C, Sun J, Nie Y, et al. High-Quality Monolayer Graphene Synthesis on Pd Foils via the Suppression of Multilayer Growth at Grain Boundaries. Small. 2014;10(19):4003-4011.
45. Zhou Z, Gao F, Goodman DW. Deposition of metal clusters on single-layer graphene/Ru(0001): Factors that govern cluster growth. Surface Science. 2010;604(13-14):L31-L38.
46. Boix V, Struzzi C, Gallo T, Johansson N, D'Acunto G, Yong Z, et al. Area-selective Electron-beam induced deposition of Amorphous-BNx on graphene. Appl Surf Sci. 2021;557:149806.
47. Hwang C, Yoo K, Kim SJ, Seo EK, Yu H, Biró LP. Initial Stage of Graphene Growth on a Cu Substrate. The Journal of Physical Chemistry C. 2011;115(45):22369-22374.
48. Zhang W, Wu P, Li Z, Yang J. First-Principles Thermodynamics of Graphene Growth on Cu Surfaces. The Journal of Physical Chemistry C. 2011;115(36):17782-17787.
49. Chen S, Gao J, Srinivasan BM, Zhang G, Sorkin V, Hariharaputran R, et al. An all-atom kinetic Monte Carlo model for chemical vapor deposition growth of graphene on Cu(1 1 1) substrate. J Phys: Condens Matter. 2020;32(15):155401.
50. Dai D, Wu M, Shu S, Yang K, Lin C-T, Han Y, et al. Thermal CVD growth of graphene on copper particles targeting tungsten-copper composites with superior wear and arc ablation resistance properties. Diamond Relat Mater. 2020;104:107765.
51. Zhang X, Zheng J, Du YQ, Wang ZW, Wu YD, Luo G. Graphene-polymer nanocomposites for thermal conductive applications. IOP Conference Series: Materials Science and Engineering. 2020;770(1):012015.
52. Chu K, Wang X-h, Wang F, Li Y-b, Huang D-j, Liu H, et al. Largely enhanced thermal conductivity of graphene/copper composites with highly aligned graphene network. Carbon. 2018;127:102-112.
53. Saboori A, Pavese M, Badini C, Fino P. Microstructure and Thermal Conductivity of Al–Graphene Composites Fabricated by Powder Metallurgy and Hot Rolling Techniques. Acta Metallurgica Sinica (English Letters). 2017;30(7):675-687.
54. Cao H, Xiong D-B, Tan Z, Fan G, Li Z, Guo Q, et al. Thermal properties of in situ grown graphene reinforced copper matrix laminated composites. J Alloys Compd. 2019;771:228-237.
55. Aliprandi A, Moreira T, Anichini C, Stoeckel MA, Eredia M, Sassi U, et al. Hybrid Copper-Nanowire–Reduced-Graphene-Oxide Coatings: A "Green Solution" Toward Highly Transparent, Highly Conductive, and Flexible Electrodes for (Opto)Electronics. Adv Mater. 2017;29(41).
56. Javidjam A, Hekmatshoar MH, Hedayatifar L, Abad SNK. Effect of surface roughness on electrical conductivity and hardness of silver plated copper. Materials Research Express. 2018;6(3):036407.
57. Dhingra S, Hsu J-F, Vlassiouk I, D'Urso B. Chemical vapor deposition of graphene on large-domain ultra-flat copper. Carbon. 2014;69:188-193.
58. Yu J, Wang L, Guan Y, Shao B, Liu Z, Zong Y. A high strength and high electrical conductivity graphene/Cu composite with good high-temperature stability. Mater Charact. 2023;201:112928.
59. Das S, Senapati S, Alagarasan D, Varadhrajaperumal S, Ganesan R, Naik R. Thermal Annealing-Induced Transformation of Structural, Morphological, Linear, and Nonlinear Optical Parameters of Quaternary As20Ag10Te10Se60 Thin Films for Optical Applications. ACS Applied Optical Materials. 2022;1(1):17-31.
60. Aparimita A, Sripan C, Ganesan R, Jena S, Naik R. Influence of thermal annealing on optical and structural properties change in Bi-doped Ge30Se70 thin films. Phase Transitions. 2018;91(8):872-886.
61. Ding W, Zhao B, Zhang Q, Fu Y. Fabrication and wear characteristics of open-porous cBN abrasive wheels in grinding of Ti–6Al–4V alloys. Wear. 2021;477:203786.
62. Petrov S, Marinova V, Lin SH, Chang CM, Lin YH, Hsu KY. Large Scale Liquid Crystal Device with Graphene-based Electrodes. Optical Data Processing and Storage. 2017;3(1).
63. Quang VV, Trong NS, Trung NN, Hoa ND, Duy NV, Hieu NV. Full-Layer Controlled Synthesis and Transfer of Large-Scale Monolayer Graphene for Nitrogen Dioxide and Ammonia Sensing. Anal Lett. 2013;47(2):280-294.
64. Zhou W, Chen C, Mikulova P, Dong M, Fan Y, Kikuchi K, et al. Thermal expansion behaviors of few-layered graphene-reinforced Al matrix composites. J Alloys Compd. 2019;792:988-993.
65. Solin NI. Room-temperature phase separation in weakly doped lanthanum manganites. Journal of Experimental and Theoretical Physics. 2005;101(3):535-546.
66. Liu P, Ng VMH, Yao Z, Zhou J, Lei Y, Yang Z, et al. Facile Synthesis and Hierarchical Assembly of Flowerlike NiO Structures with Enhanced Dielectric and Microwave Absorption Properties. ACS Applied Materials and Interfaces. 2017;9(19):16404-16416.
67. Liu P, Peng J, Chen Y, Liu M, Tang W, Guo Z-H, et al. A general and robust strategy for in-situ templated synthesis of patterned inorganic nanoparticle assemblies. Giant. 2021;8:100076.
68. Temir A, Zhumadilov KS, Zdorovets MV, Korolkov IV, Kozlovskiy A, Trukhanov AV. Synthesis, phase transformations, optical properties and efficiency of gamma radiation shielding by Bi_2O_3-TeO_2-WO_3 ceramics. Opt Mater. 2021;113:110846.
69. Zeng M, Fu L. Controllable Fabrication of Graphene and Related Two-Dimensional Materials on Liquid Metals via Chemical Vapor Deposition. Acc Chem Res. 2018;51(11):2839-2847.
70. Yang Y-J, Zhang B, Wan H-Y, Liu K, Zhang G-P. Bilayer graphene-covered Cu flexible electrode with excellent mechanical reliability and electrical performance. J Mater Res. 2019;34(21):3645-3653.
71. Naik RB, Reddy KV, Reddy GM, Arockia Kumar R. Development of high strength and high electrical conductivity Cu/Gr composites through friction stir processing. Mater Lett. 2020;265:127437.
72. Cao M, Luo Y, Xie Y, Tan Z, Fan G, Guo Q, et al. The Influence of Interface Structure on the Electrical Conductivity of Graphene Embedded in Aluminum Matrix. Advanced Materials Interfaces. 2019;6(13).
73. Mohan VB, Lau K-t, Hui D, Bhattacharyya D. Graphene-based materials and their composites: A review on production, applications and product limitations. Composites Part B: Engineering. 2018;142:200-220.
74. Luechinger NA, Athanassiou EK, Stark WJ. Graphene-stabilized copper nanoparticles as an air-stable substitute for silver and gold in low-cost ink-jet printable electronics. Nanotechnology. 2008;19(44):445201.
75. Sahoo D, Alagarasan D, Ganesan R, Varadharajaperumal

S, Naik R. Impact of irradiation doses on the structural, morphological, and linear–nonlinear optical properties of Ge10Sb25Se65 thin films for optoelectronic applications. The European Physical Journal Plus. 2022;137(6).
76. Sahoo D, Sahoo S, Alagarasan D, Ganesan R, Varadharajaperumal S, Naik R. Proton Ion Irradiation on As40Se50Sb10 Thin Films: Fluence-Dependent Tuning of Linear–Nonlinear Optical Properties for Photonic Applications. ACS Applied Electronic Materials. 2022;4(2):856-868.
77. Mudgal N, Saharia A, Choure KK, Agarwal A, Singh G. Sensitivity enhancement with anti-reflection coating of silicon nitride (Si_3N_4) layer in silver-based Surface Plasmon Resonance (SPR) sensor for sensing of DNA hybridization. Appl Phys A. 2020;126(12).
78. Parida A, Alagarasan D, Pradhan GK, Naik R. Time dependent 532 nm laser irradiation on quaternary Sb10S15 In15Se60 films: An insight into its structural, morphological, and optical modifications for photonics application. Physica B: Condensed Matter. 2023;657:414785.
79. Priyadarshini P, Senapati S, Bisoyi S, Samal S, Naik R. Zn doping induced optimization of optical and dielectric characteristics of CuInSe2 nanosheets for optoelectronic device applications. J Alloys Compd. 2023;945:169222.
80. Naik R, Ganesan R, Sangunni KS. Optical properties change with the addition and diffusion of Bi to As2S3 in the Bi/As_2S_3 bilayer thin film. J Alloys Compd. 2013;554:293-298.
81. Naik R, Ganesan R, Sangunni KS. Photo induced optical changes in Sb/As2S3 multilayered film and (As2S3)0.93Sb0.07 film of equal thickness. J Alloys Compd. 2010;505(1):249-254.
82. Vlassiouk I, Regmi M, Fulvio P, Dai S, Datskos P, Eres G, et al. Role of Hydrogen in Chemical Vapor Deposition Growth of Large Single-Crystal Graphene. ACS Nano. 2011;5(7):6069-6076.
83. Chen X, Zhang L, Chen S. Large area CVD growth of graphene. Synth Met. 2015;210:95-108.
84. Antonova IV. Chemical vapor deposition growth of graphene on copper substrates: current trends. Physics-Uspekhi. 2013;56(10):1013-1020.
85. Li X, Cai W, An J, Kim S, Nah J, Yang D, et al. Large-Area Synthesis of High-Quality and Uniform Graphene Films on Copper Foils. Science. 2009;324(5932):1312-1314.
86. Lim H, Lee HC, Yoo MS, Cho A, Nguyen NN, Han JW, et al. Effects of Hydrogen on the Stacking Orientation of Bilayer Graphene Grown on Copper. Chem Mater. 2020;32(24):10357-10364.
87. Li P, Li Z, Yang J. Dominant Kinetic Pathways of Graphene Growth in Chemical Vapor Deposition: The Role of Hydrogen. The Journal of Physical Chemistry C. 2017;121(46):25949-25955.
88. Lin L, Deng B, Sun J, Peng H, Liu Z. Bridging the Gap between Reality and Ideal in Chemical Vapor Deposition Growth of Graphene. Chem Rev. 2018;118(18):9281-9343.